Received: 1 February 2023 | Revised: 20 March 2023 | Accepted: 16 April 2023

DOI: 10.1111/ijac.14421

International Journal of Applied Ceramic Technology

RESEARCH ARTICLE

Designing slurry conditions to control size distribution of spray-dried dense YSZ granules

Hyun-Ae Cha[1,2] | **Kyung-Chan Shin**[2] | **Hee-Jin Son**[2] | **Byung-Dong Hahn**[2] | **Cheol-Woo Ahn**[2] | **Jong-Jin Choi**[2] | **Do Kyung Kim**[1]

[1]Department of Materials Science and Engineering, Korea Advanced Institute of Science and Technology (KAIST), Daejeon, Republic of Korea

[2]Department of Functional Ceramics, Ceramic Materials Division, Korea Institute of Materials Science (KIMS), Changwon, Republic of Korea

Correspondence
Jong-Jin Choi, Department of Functional Ceramics, Ceramic Materials Division, Korea Institute of Materials Science (KIMS), 797 Changwon-daero, Seongsan-gu, Changwon 51508, Republic of Korea.
Email: finaljin@kims.re.kr

Do Kyung Kim, Department of Materials Science and Engineering, Korea Advanced Institute of Science and Technology (KAIST), 291 Daehak-ro, Yuseong-gu, Daejeon 34141, Republic of Korea.
Email: dkkim@kaist.ac.kr

Funding information
Ministry of Trade, Industry & Energy (MOTIE), Grant/Award Number: 20011008; Korea Institute of Materials Science (KIMS) internal R&D program, Grant/Award Number: PNK8140

Abstract

This study suggests approaches to achieve the desired size and size distribution of highly dense spherical granules by investigating the effect of slurry conditions on size distribution. Highly dense spherical granules were prepared with a solid content of over 77 wt% by spray-drying the slurry. A prolonged deagglomeration time of 64 h provided adequate flowing ability by breaking up almost all aggregates and improved dispersibility, resulting in reduced granule sizes and narrow size distributions. The optimum slurry conditions for maintaining dispersibility were 1 wt% of the dispersant and a strong basic pH, which had the greatest effect on size distribution. Based on these considerations, the 10.6 μm sized 3 mol% yttria-stabilized zirconia granules were synthesized with 99.83% density, 97.17% sphericity, and uniform size with fraction yield of 80.01% at 10–20 μm. These dense granules have significantly higher hardness and modulus values of 19.19 and 206.68 GPa, respectively, than that of pellet and film types. To the best of our knowledge, the relationship between the slurries and the span of the size distribution of ceramic granules during spray-drying has been demonstrated for the first time.

KEYWORDS
mechanical properties, particle size distribution, slurry optimizing, spray-drying, yttria-stabilized zirconia

1 | INTRODUCTION

Yttria-stabilized zirconia (YSZ) is widely used as a standard material in thermal barrier coatings because of its low thermal conductivity,[1] dental restoration owing to its excellent mechanical strength,[2] and applications, such as grinding and milling media, requiring high density with uniform size and sphericity.[3] Recently, the demand for ultrasmall (less than 30 μm) beads, which are smaller in size than existing ceramic beads, has been rapidly increasing for the nano-miniaturization of core raw material powders and integration of parts in various high-tech industries, such as electricity/electronics, energy, and environment.[4,5] In particular, nano-miniaturization and high-purity raw material powders are necessary for the high performance of multilayer ceramic capacitors. Therefore, the size of the required beads has been gradually reduced, and a higher hardness is required than before to withstand strong impact. There is a technical limitation in manufacturing ultrasmall ceramic beads using the existing ceramic bead

manufacturing process. In addition to simply making the bead size small, it should be possible to impart high hardness and high-density characteristics to the ceramic beads themselves so as to impart to the material to be pulverized high purity and miniaturization. It is also important to achieve precise size control and high sphericity. Therefore, research on controlling the size of spherical YSZ to a small size with high mechanical strength and density is important. Furthermore, because the method of classifying and supplying ceramic beads with a wide particle size has to be price competitive, developing a processing method for ceramic particles that satisfy the required characteristics in a single size is necessary.

Controlled wet processing is an important step in ceramic manufacturing and significantly impacts the morphologies and properties of all intermediate and final products in ceramic manufacturing, including spray-drying.[6–15] Granulation is an essential step in improving the flowability of submicron and nano-ceramic powders to make them suitable for industrial processing.[16,17] Controlling the average granule size and size distribution is important in granulation processes. Spray-drying is a method of fabricating ceramic granules by which a water-based suspension (slurry) is changed to a dry, free-flowing spherical powder (granules) by rapidly spraying the feeding slurry into a stream of heated gas for drying.[18–20] The main parameters affecting the shape and size distribution of spray-drying technology are slurry properties (concentration, viscosity, stability, and properties of initial particles) and process parameters (atomizing pressure of spraying gas, temperature, feed rate, and nozzle diameter).[21–24]

Therefore, the effects of slurry conditions on the properties of spray-dried ceramic granules were studied. Most studies have focused on the effect of slurries on the morphology and final product properties of granules.[9,25–27] For example, concerning the spray-drying of alumina, a correlation was established between the slurry characteristics and the morphologies of the granules; a flocculated slurry is prone to producing smaller and dimpled granules.[28] In addition, the condensing degree of the granules can be affected by the moisture content and stability of the slurry, indicating that the density of the green body can be changed by the slurry, resulting in the slurry properties indirectly controlling the structure and properties of the sintered body.[12] Coddet et al. established a stability map showing stable regions for controlling the morphology of zirconia granules based on the amount of dispersant and binder depending on the sedimentation height using a single droplet drying device.[29–31]

Few researchers have focused on the technology for producing 10 μm class granules via spray-drying. Most studies have produced an average granule size of over 50 μm and exhibited a wide size distribution (~50 μm or greater spread) (Table S1). Our research group succeeded in fabricating highly dense YSZ ceramic granules of size 20–30 μm by controlling the structural features of the supraparticle, such as sphericity and micromechanical properties, by adjusting the spray-drying process parameters.[7] However, the yield of the desired particle size was approximately 20% because only the process parameters of spray-drying were applied, without considering the particle size distribution. Previous studies have attempted to understand the effect of spray-drying process variables and the relationship between the properties of the slurry and the morphology of the granules. The direct relationship between the properties of the slurry and the size, including the distribution of the granules, has yet to be adequately studied because the spraying process parameter has a more significant effect on the size change. However, to make 10 μm class granules with uniform size, it is imperative to not only control the spraying process parameters but also finely optimize the slurry conditions. Therefore, acquiring highly dense ultrasmall YSZ granules with a spherical morphology and a narrow size distribution while achieving mechanical strength is crucial, yet challenging. It is particularly difficult to achieve a uniform granule size with a breakthrough yield of the desired size.

Herein, we report the highly dense 10 μm size of 3 mol% YSZ granules with a high yield fraction of over 80% by controlling the slurry conditions. To the best of our knowledge, this is the first study to demonstrate the relationship between slurries and the size distribution of ceramic granules during spray-drying. We also examined the modification of the shape of the granules. Here, we present four approaches to these objectives: (i) preparing high-concentration YSZ-based aqueous suspensions considering the viscosity, density, spherical morphology, and size distribution of sintered granules; (ii) investigating the influences of deagglomeration time on the flowing ability of slurry and the size distribution of granules, and the effect of atomizing pressure on the size change; (iii) studying the dispersing ability of the slurry according to the amount of dispersant and pH to determine suitable stabilization conditions; and (iv) acquiring 10 μm class YSZ granules with superior sphericity, narrow size distribution, and excellent mechanical strength by optimizing the spray-drying conditions.

2 | EXPERIMENTAL PROCEDURES

2.1 | Materials

In this study, zirconia powder containing 3 mol% yttria was used (average particle size: 4.68 μm, supplied by CENOTEC, Korea). High-purity α-alumina powder

(AKP-30, Sumitomo, Japan) was added within the solubility limit to prevent abnormal grain growth and act as a sintering aid.[32] To achieve well-stabilized and well-dispersed zirconia slurries, an ammonium polycarboxylate dispersant (San Nopco, SN-DISPERSANT 5468) was added. The pH was adjusted using diluted solutions of hydrochloric acid (HCl, 1 N, Samchun Chemicals, Korea) or sodium hydroxide solution (NaOH, 1 N, Samchun Chemicals, Korea).

2.2 | Slurry preparation

The slurry was prepared with various conditions, including solid contents (65.25–80.25 wt%), time of ball-mill treatment (1–64 h), dispersant amount (0.5–2 wt%), and pH (5.5–10.5), to investigate the stable and appropriate conditions for 10 μm class granule size. The slurry was composed of 3 mol% YSZ (65–80 wt%), Al_2O_3 (0.25 wt%), dispersant (0.5–2 wt%), and distilled water (17.75–32.75 wt%), so that the ratio of the ceramic powder/slurry was 65.25–80.25 wt%. The mixture was ball-milled using 2 mm balls that were 5/3 the weight of the slurry in a polyethylene bottle under controlled pH conditions.

2.3 | Spray-drying and sintering process

Spray-drying of the suspensions was carried out in a two-fluid nozzle spray-dryer (SD 1010, EYELA, Japan), and the setting parameters were established by referring to our previous experiments.[7] The inlet and outlet stream temperatures were maintained at 110 and 70–80°C, respectively. Furthermore, the feed rate and drying airflow were fixed at 600 mL/h and 0.64 m^3/min, respectively. The conditions of atomizing pressure (100–250 kPa N_2 gas pressure) were changed to investigate the effect of reducing the size of the granules. The sprayed and dried powders were sieved with mesh sizes of 10, 20, 25, 32, 45, and 75 μm to determine the fraction yield efficiency. The sieved powder was sintered in an alumina crucible at 1400°C for 80 min at a heating rate of 2°C/min.

2.4 | Characterizations

The microstructures of the YSZ granules were analyzed using field-emission scanning electron microscopy (SEM, IT300, JEOL, Japan). Granule size distributions were determined by static light scattering using a particle size analyzer (LS320, Beckman Coulter Inc., USA). Granule density was measured using a gas pycnometer (BELpycno, MicrotracBEL Corp., Japan). The viscosity changes of the slurries at 100 rpm were characterized using a viscometer (DV-II, Brookfield, USA) with spindle No. 64, and the zeta potential was determined using dynamic light scattering (Malvern ZS Nano S analyzer, Malvern Instrument Inc., London). In addition, the stability of each sample was analyzed by measuring the backscattering (BS) every hour in a Turbiscan Lab apparatus (Formulaction, France) at 25°C. Turbiscan carried out step-by-step vertical scanning of the whole sample using a pulsed near-infrared light source ($\lambda = 850$ nm) and converted the macroscopic aspects of the mixtures into graphics. Backscatter data acquisition from the backscatter detector received light backscattered by the sample at 135° from the incident beam.[33]

Mechanical testing was performed using nanoindentation. Before the nanoindentation tests, the granules were embedded in a black epoxy resin (Struers, DuroFast, Denmark). The molten resin was then hot pressed ($F = 10$ kN and $T = 180$°C for 10 min). The surfaces of the granules were polished to a roughness of 2 μm using a sequence of ultrafine 1000, 2000, and 4000 grit SiC papers. The surface roughness of the mounted specimens was analyzed using a 3D measuring laser microscope (Olympus OLS5000 LEXT). The mechanical tests were performed in an Anton Paar nanoindenter (NHT3, Anton Paar, Austria) system with a load of 5–20 mN using a diamond Berkovich tip (angle of 142.3° and tip roundness of $r \leq 100$ nm) indenter. The loading and unloading rates were both 10.0 Hz, and the holding time at the maximum load was 3 s. The average hardness and elastic modulus values were determined from 10 indentation experiments.

3 | RESULTS AND DISCUSSION

3.1 | The effect of solid contents

Spray-drying was performed with solid contents of 65.25, 75.25, 77.25, and 80.25 wt%. Figure 1 shows the YSZ granules spray-dried at different solid contents. The drying temperature was controlled by adjusting the inlet temperature of the spray-drying process, which appropriately controlled the drying kinetics. For the formation of high-density ceramic granules, the evaporation velocity of the water solvent was optimized to be slower than the diffusion rate during mass transfer, generating highly dense granules by the isotropic shrinkage of liquid droplets. Therefore, spray-drying was carried out at inlet and outlet stream temperatures of 110 and 70–80°C, respectively. Meanwhile, owing to the high moisture content at a solid content of 65.25 and 75.25 wt%, less-dried granules easily merge during the drying process; thus, the morphology presents poor sphericity.

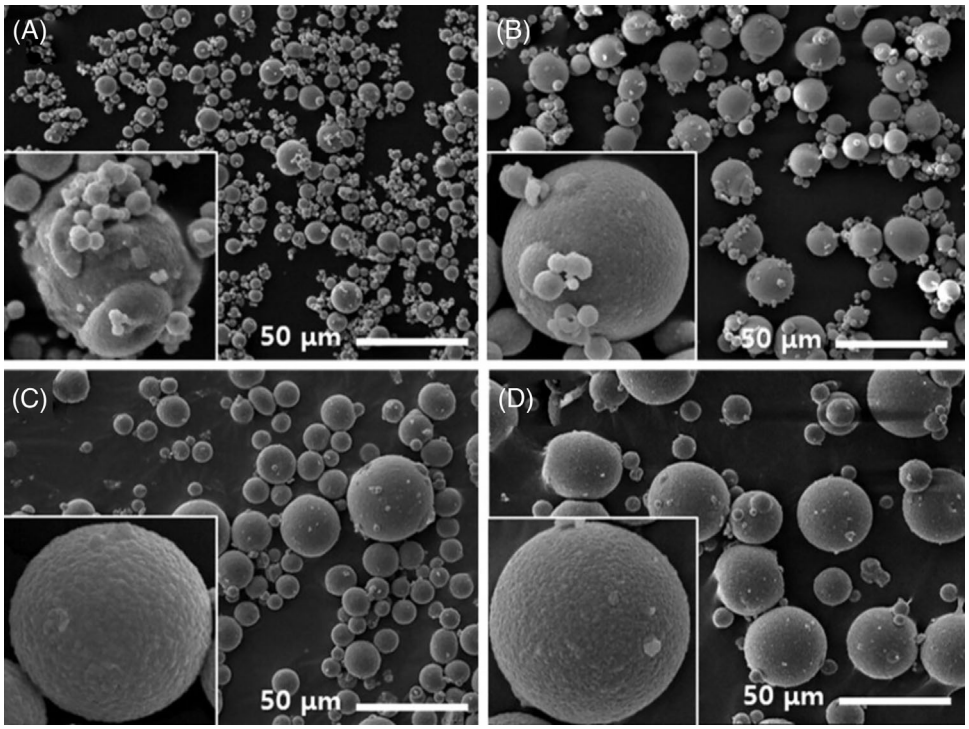

FIGURE 1 Scanning electron microscopy (SEM) micrographs of sintered granules with various solid contents of (A) 65.25 wt%, (B) 75.25 wt%, (C) 77.25 wt%, and (D) 80.25 wt% after sintering.

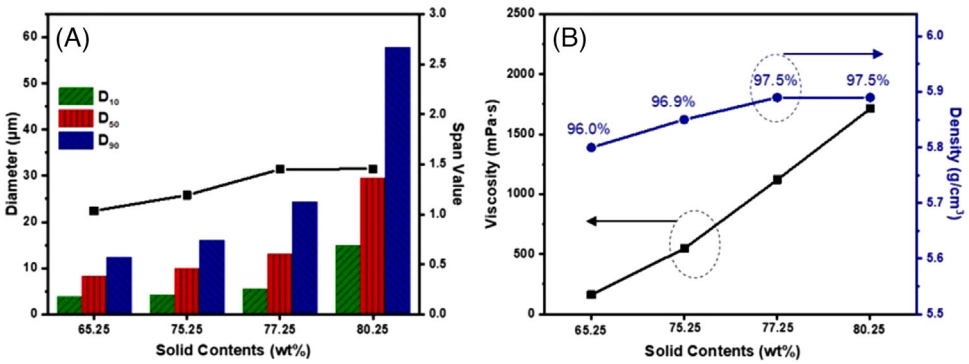

FIGURE 2 (A) D_{10}, D_{50}, D_{90}, and span values of sintered granules; (B) viscosity of slurry and density of sintered granules with various solid contents.

The concentration of the slurry, which depends considerably on the solid content, is an important parameter that determines the size of the dried granules. In Figure 2A, as the solid contents increase from 65.25 to 80.25 wt%; there is a tendency for D_{10}, D_{50}, and D_{90} to increase from 3.91, 8.25, and 12.43 to 14.97, 29.51, and 57.84 μm, respectively. To define the distribution width, the span of the volume-based size distribution is defined as

$$Span\ value = \frac{D_{90} - D_{10}}{D_{50}} \quad (1)$$

A higher value indicates a wider particle size distribution. Owing to the relatively small increase in D_{10} compared to D_{50} and D_{90}, the span value increased with the increase in solid content up to 77 wt%. In particular, at the point of change from 77.25 to 80.25 wt%, D_{10}, D_{50}, and D_{90} increase significantly overall, and the span value remains constant. This result reveals that the solid contents had a significant effect on the particle size and size distribution and shows that solid contents of 80.25 wt% are not suitable for 10 μm granules.

The higher concentration of solids in the feeding slurry resulted in higher viscosity, as shown in Figure 2B.

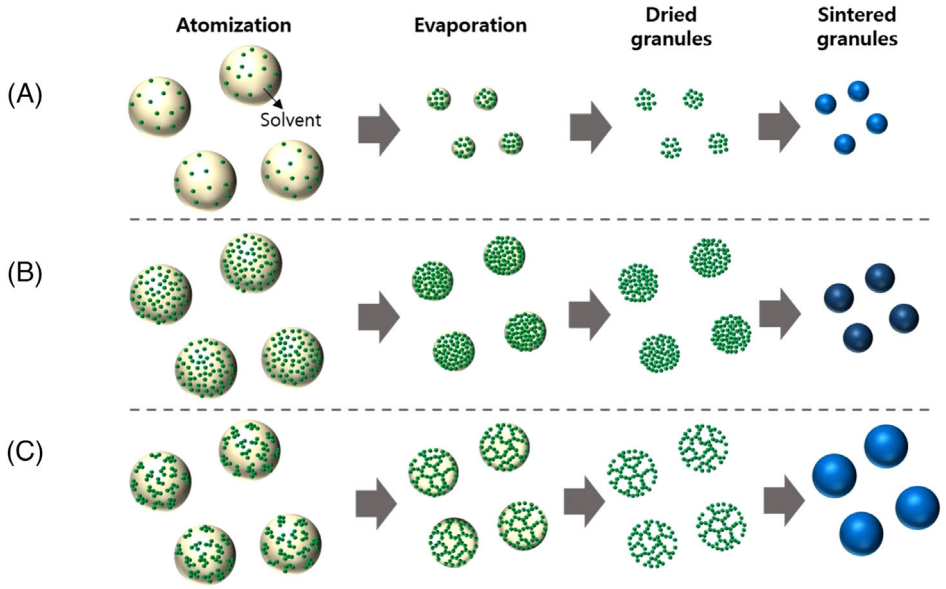

FIGURE 3 (A) Low solid contents; (B) High solid contents; (C) High & Agglomerated solid contents. Shematic illustration of the effect of the conditions of slurry contents on the size and density of the dried granule with a slower evaporation velocity of water solvent than diffusion rate.

Consequently, when a feeding slurry with a high solid content is atomized, large droplets dry into large granules. This is because they shrink less when the liquid evaporates compared to droplets produced from a feeding slurry with low solid content, as shown in Figure 3A,B. In contrast, at low solid contents, there were smaller droplets and more shrinkage, resulting in a smaller granule size. This relationship can also be expressed by the following equations that describe the droplet size and geometric diameter of the dry particles[18,20]:

$$D_d = \alpha \left(\frac{\sigma^s \rho_L^{t1} \eta^r}{\rho_A^{t2}} \right) \left(\frac{f_L}{f_L v_L + f_A v_A} \right) \tag{2}$$

$$D_g = \sqrt[3]{\frac{C_F}{\rho_P}} D_d \tag{3}$$

where D_d and D_g are the average diameter of the droplet and geometric diameter of the dried granule after the spray-drying process, respectively. α is a constant that depends on the spray design, ρ is the density, η is the viscosity, σ is the surface tension, f is the flow rate, and v is the velocity of the liquid (L) and the atomization gas (A). s, t, and γ are constants, the values of which depend on operating conditions. C_F is the concentration of the feed slurry, and ρ_P is the droplet particle density. The above formulas indicate that the particle size is also directly affected by changes in concentration, varying with the solid content of the feed solution. As the solid content increased, D_d increased because the viscosity and density of the liquid increased, whereas the other variables remained constant. The geometric diameter also increased with an increase in D_d and feed slurry concentration.

As shown in Figure 2B, all the solid contents have a high density of over 96% of the relative density (theoretical density: 6.04 g/cm^3)[2] due to the relatively high solid contents of over 65.25 wt%. Among the conditions, the density of the sintered granules showed the highest value at a solid content of 77.25–80.25 wt%, along with good sphericity. To optimize the conditions for the 10 μm class of YSZ granules with relatively superior yield, sphericity, and mechanical properties, the following research was conducted with 77.25 wt% solid contents.

3.2 | Effect of deagglomeration time

Figure 4 shows the viscosity of the slurry, the density of sintered granules, size distribution after sintering, and morphology of dried granules to investigate the influence of the degree of deagglomeration on the flow behavior of a slurry containing 77.25 wt% solid content according to the ball-milling time. As shown in Figure 4A, the initial viscosity at 1 h was relatively low. In the initial ball-milling stage of less than 1 h, the powder seemed to agglomerate into large clumps, resulting in the formation of large oval granules approximately 50 μm in size after spray-drying (Figure 4D). Subsequently, the viscosity increased from 1 to 4 h, likely because the size of the powder was significantly reduced from the initial size owing to a weak connection between the initial particle clumps and decreased

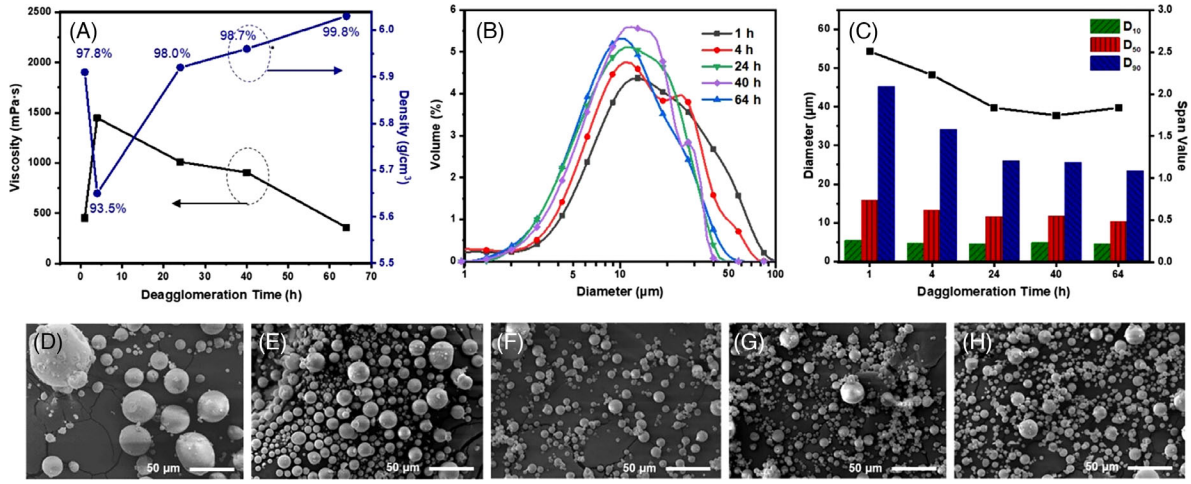

FIGURE 4 (A) Viscosity of slurry and density of sintered granules with various solid contents; (B) size distributions of granules obtained by different deagglomeration times; (C) D_{10}, D_{50}, D_{90}, and span values of the sintered granules. Scanning electron microscopy (SEM) micrographs of spray-dried granules with a deagglomeration time of (D) 1, (E) 4, (F) 24, (G) 40, and (H) 64 h.

polydispersity of the particles. A smaller particle size results in a higher number of particles in a given volume, and as a result, the particle surface area can be orders of magnitude higher than the initial one, leading to greater interactions between particles and increased viscosity. Additionally, the size distribution of the particles is narrower, which may result in less efficient packing compared to particles with a larger distribution. It means that less free space is available in the case of narrow distribution for individual particles to move around, making sample flow less easily. Furthermore, the time is not enough for the complete spreading of the dispersant in this position. As a result, during the initial period when the powder size and size distribution reduced rapidly, the suspension's viscosity can be increased. This speculation can be further confirmed by the change in the size distribution of the granules after sintering, as shown in Figure 4B. The granules spray-dried after deagglomerating for 1 h showed one primary population of fine particles centered at approximately 11 μm and a secondary, smaller population of coarse particles centered at approximately 50 μm owing to the initial conglomerated particles. As the deagglomeration time increased, the population of coarse particles diminished, and the size of the fine particles was reduced, suggesting that the clumped raw powders were destroyed. Therefore, as shown in Figure 4C, the span value decreases until the coarse particles disappear after 24 h.

In addition, extending the deagglomeration time from 4 to 64 h significantly reduced the viscosity, suggesting a distinctive improvement in the fluidity of the suspension. Specifically, part of the liquid trapped inside the network structure is released, a more ordered structure is formed, and the dispersant is distributed evenly and well. Meanwhile, the particle size and size distribution of the spray-dried granules did not change significantly as the deagglomeration time increased from 24 to 64 h, as shown in Figure 4C, because the agglomerates of the initial particles were almost completely broken after 4 h. The change in viscosity due to the reduction in particle size and size distribution is insignificant, likely because the change in particle size is small. However, it appears that the dispersant is uniformly dispersed, and the dispersibility seems to improve with increasing ball mill time. Consequently, a uniform structure was formed in the slurry, and its flowing ability further improved, resulting in fine granules, as shown in Figure 4F–H. This size distribution result follows Equation (2), which shows the proportionality between viscosity and droplet size.

The density displays an opposite trend to that of the viscosity, as shown in Figure 4A. It is believed that the large clumps of the initial particles are strongly agglomerated during drying so that the spray-dried granules show a high density of 97.8% at 1 h. At a deagglomeration time of 4 h, the density decreased because of the agglomerated solid content and low dispersibility and fluidity of the suspension, which occurred when the initial large clumps began to break up, as shown in Figure 3C. At the 24 h stage, almost all agglomerates of the initial powder disappeared, and the well-dispersed slurry with an ordered structure had denser particle packing within the granules compared to the initial condition (Figure 3B). As the time increased up to 64 h, the density reached 99.8% (6.03 g/cm^3).

3.3 | Effect of atomizing pressure

Atomizing pressure is one of the major variables governing granule size in spray-dry process settings. The

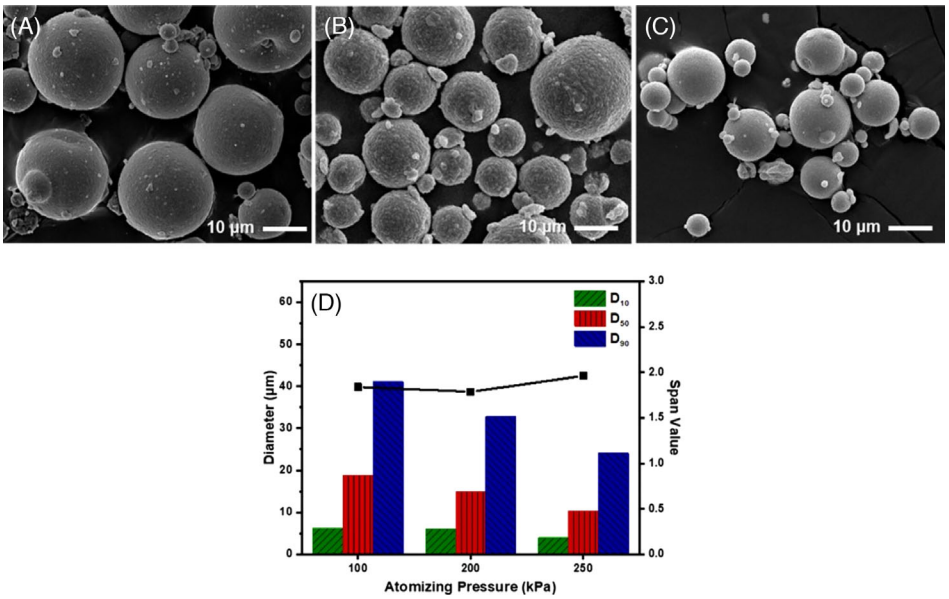

FIGURE 5 Scanning electron microscopy (SEM) micrographs of spray-dried granules after sintering at each atomizing pressure: (A) 100, (B) 200, and (C) 250 kPa; (D) D_{10}, D_{50}, D_{90}, and span values of the sintered granules at each atomizing pressure.

average droplet size was inversely proportional to the atomizing energy.[18] Figure 5 shows the morphology and size distribution of the granules at atomizing pressures of 100, 200, and 250 kPa. When gas collides with the surface of the liquid at a high atomizing pressure, the liquid accelerates and shrinks. Conversely, the atomization energy was reduced at lower pressures, resulting in larger droplets, and the final dried granules were larger in size. This finding is consistent with the literature on spray-dried hydroxyapatite[34,35] and metal powders.[25,36] The span value, which depends on the atomizing pressure, is consistent because of the size change at a constant rate, as shown in Figure 5D. In addition, the effect of the nozzle diameter was checked, but there was no effect on the size change of the granules acquired from the cyclone chamber, depending on the nozzle diameters of 0.71 and 0.41 mm (Figure S1). For forming 10 μm sized granules, the highest atomizing pressure of 250 kPa allowed in the equipment is more suitable. However, for the formation of uniform granules with a low span value of approximately 10 μm, the slurry conditions, such as stability, should be modified, as shown in the following results.

3.4 | Influence of dispersant amount and pH on the stability of slurry

As shown in Figure 3B,C, for small-sized granules, the deagglomeration of the particles in the slurry should be maintained; the stability of the slurry is extremely important for ultrasmall granules. To determine the suitable amount of dispersing agent, the zeta potential and viscosity

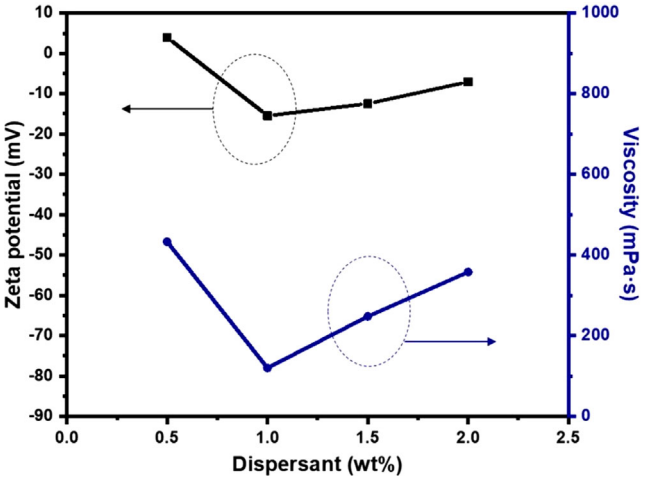

FIGURE 6 Effect of dispersant amounts on the zeta potential and viscosity of slurry.

of the slurry were measured ranging from 0.5 to 2 wt%, as shown in Figure 6. The value of the zeta potential indicates the possible behavior of the dispersion, and a high value is related to suspension stability. At the isoelectric point (IEP) of the powder at which the electrokinetic surface charge of the particle is zero, the attractive interaction between particles is not countered, and the suspension achieves its most flocculated state. Consequently, it is expected that the surface charge of YSZ in the region far from the IEP value is sufficient to induce a repulsive force between the particles to maintain the slurry in a dispersed state. The amount of dispersant that provides optimum potential stability with the lowest zeta potential has the lowest viscosity at a

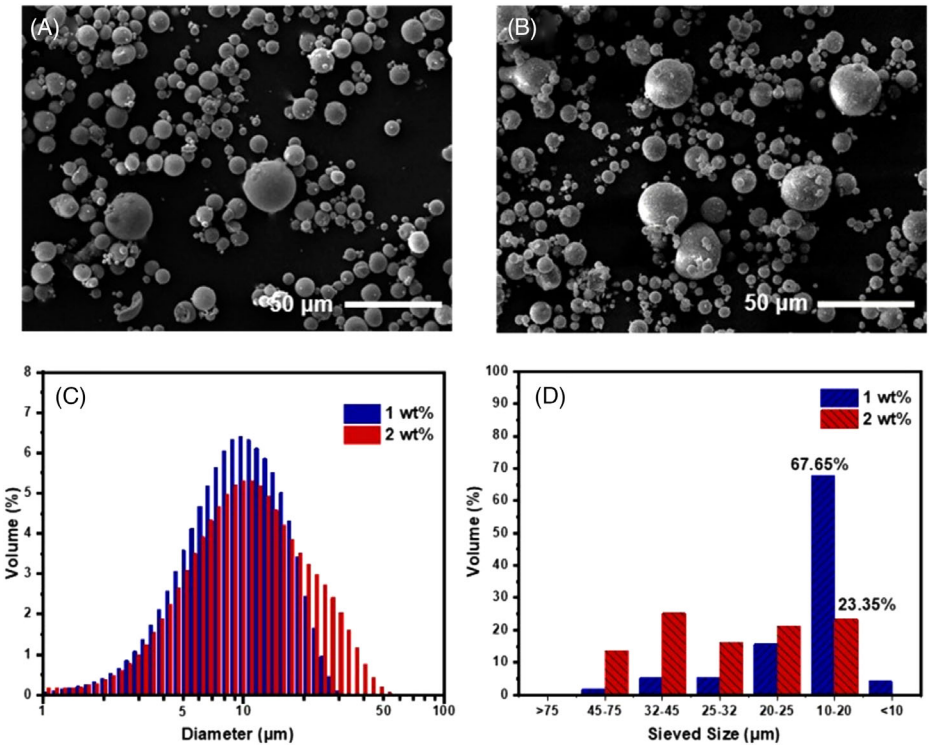

FIGURE 7 Scanning electron microscopy (SEM) micrographs of sintered granules after sintering with (A) 1 and (B) 2 wt% dispersant amount; (C) size distributions and (D) fraction yield of granules on each sieve opening size after sieving obtained by 1 and 2 wt% of dispersant amount.

dispersant amount of 1 wt%. It appears to have a low viscosity because the powder is spread with strong repulsion at the part with the lowest zeta potential. This shows that there is a correlation between the viscosity and amount of dispersant. Thus, it can be inferred that 1 wt% dispersant is the optimum amount to disperse and stabilize the slurry. Determining the optimal dispersant amount is important for improving the potential stability of the slurry and enhancing the efficiency of the deagglomeration process.

Figure 7 presents the results of the SEM micrograph, size distribution, and fraction yield after classifying the sintered granules using different sieve sizes, with 1 and 2 wt% of dispersant amounts while all other experimental conditions remain constant. For the optimized dispersant amount of 1 wt%, clear differences were detected in the size distribution with a narrow graph after sintering compared with 2 wt%, as shown in Figure 7C. Additionally, the yield for 10–20 μm during the sieving process with dry granules significantly increased from 23.35% with a 2 wt% dispersant amount to 67.65% with a 1 wt% dispersant amount, in Figure 7D.

To determine the optimal pH for the slurry with 1 wt% dispersant, the effect of pH on the zeta potential was investigated, as shown in Figure 8A. Because of the weakly acidic dispersant and raw material powder, the slurry prepared without pH adjustment had a pH of 6.5. Usually, the zeta potential farthest from the IEP with a stable pH zone is found in the alkaline part.[5,23] This is because the anionic polyelectrolyte dispersant at an acidic pH significantly reduces the degree of dissociation of the deflocculant, thus reducing its adsorption efficiency. As expected, the zeta potential was over 30 mV at a pH of 8 or more, and a well-dispersed slurry was obtained. This observation is further proven by the Turbiscan Lab Expert stability analyzer investigating the stability of the slurry at pH 6.5, 8.5, and 10.5, as shown in Figure 8B–D. Turbiscan is a potentially promising method for studying stability over a short period while simultaneously providing information on destabilization kinetics, including purification, coalescence, agglomeration, and sedimentation.[33,37] Based on the variation in the droplet volume fraction (migration) or average size (coalescence), variation of the BS signals measured as a function of time was performed along the cylindrical cell every 10 min for 12 h. At pH 6.5, there is a significant change in delta BS, which forms at a height slightly above the floor due to rapid sedimentation and flocculation. However, only slight sedimentation occurred at pH 8.5. Because of the improved dispersion stability of the slurry, the thickness of the sedimentation layer also decreased as the pH increased to 10.5. From this result, the pH of the stabilized slurry was determined to be 10.5.

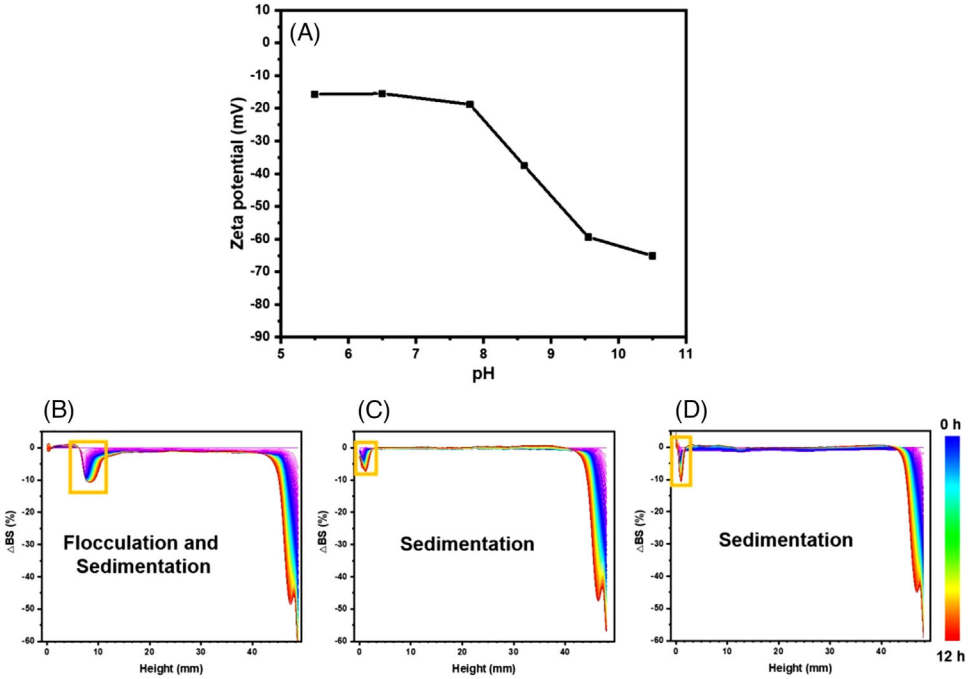

FIGURE 8 (A) Effect of pH on zeta potential of slurry: (B–D) the Turbiscan profiles showing delta backscattering as a function of time (0:00–12:00 h) at pH (B) 6.5, (C) 8.5, and (D) 10.5, respectively.

3.5 | The characterization and mechanical strength of 10 μm YSZ granules

Figure 9A,B shows the morphologies of the granules after sintering and sieving with a 10–20 μm mesh at optimized slurry conditions (solid contents of 77.25 wt%, deagglomeration time of 64 h, 1 wt% dispersant amount, and pH 10.5), and atomizing conditions at 250 kPa based on the above experimental results. Figure S2 shows the X-ray diffraction results of the YSZ raw powder and YSZ granules before and after sintering, where the monoclinic phase was transformed to the tetragonal phase after sintering. The average diameter of the granules was 10.6 μm with a uniform size, varying by only 1.84 μm using ImageJ software. Sphericity was calculated by measuring the radius of 100 granules, using the following equation:

$$Sphericity\ (\%) = \frac{d_s}{d_L} \times 100 \tag{4}$$

where d_s is the ratio of the maximum axial length, and d_L is the minimum axial length of a particle. The calculated sphericity showed an excellent value of 97.17%.[38] In addition, the D_{50} of the size distribution after sieving with a 10–20 μm mesh had similar results with an average of 10.18 μm, as shown in Figure 9C. Under these conditions, the fraction yield after sieving at 10–20 μm was 80.01%, a 40% increase over the conditions before controlling the pH (Figure 7D, 67.65%). Figure 10 shows the effects of slurry stability on granule size and size distribution. The large size distribution was significantly reduced compared with the results before the dispersant amount and pH conditions were adjusted. A better dispersed slurry could be used to fabricate smaller granules of uniform size. The span value was significantly reduced by optimizing the slurry conditions.

Consequently, the desired 10 μm YSZ granules with superior sphericity and extremely high yield efficiency were synthesized by carefully considering the slurry preparation parameters and spray-drying setting parameters. The mechanical properties of the fabricated YSZ granules were analyzed by nanoindentation, as shown in Figure 11. In nanoindentation, a diamond tip is pressed into the specimen to given maximum depth or load and then removed. Simultaneously, the load and displacement of the indenter were also recorded. From such a load–depth curve, the hardness (H) and Young's modulus (E) of the specimen can be analyzed using the Oliver and Pharr method.[39] The Poisson ratio of YSZ is 0.25,[40] which is needed to determine Young's modulus. For an accurate measurement, the surface of the polished specimens was checked using the 3D surface roughness analysis technique, and the value was less than 2 μm (Figure 11A).

At different nanoindenter loads, the hardness and elastic modulus were analyzed to investigate the optimal conditions for the nanoindentation test. The highest hardness is observed at 10 mN. When the load was increased to 20 mN, the elastic modulus increased, but the hardness decreased;

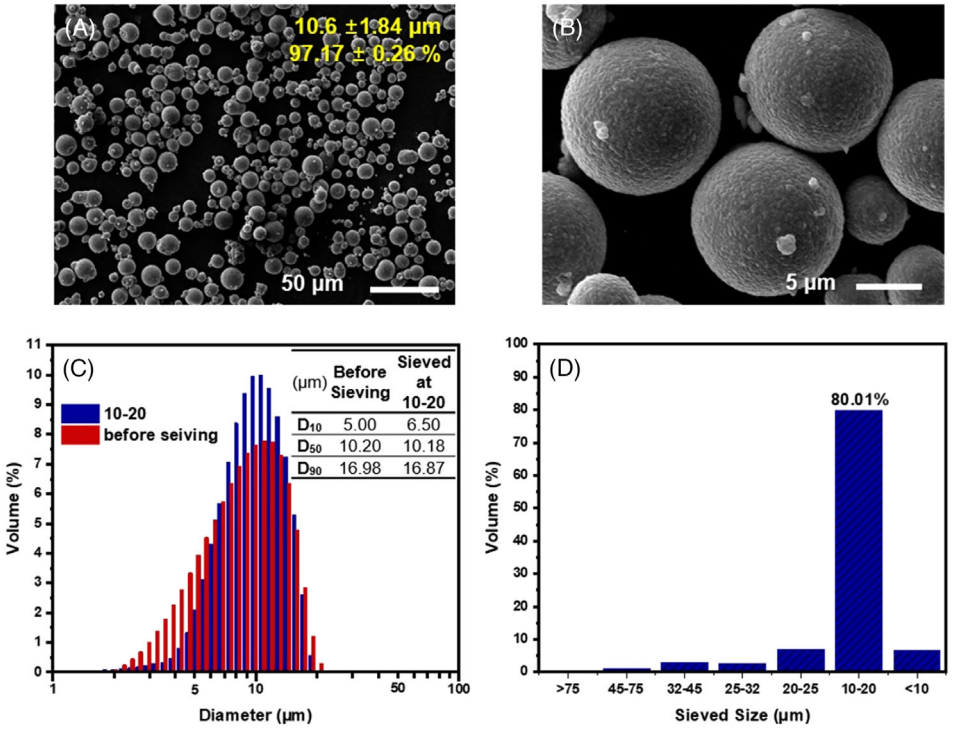

FIGURE 9 (A and B) Scanning electron microscopy (SEM) micrographs of sintered granules with the optimized condition for 10 μm class granules; (C) size distributions before and after sieving 10–20 μm, and (D) fraction yield of granules on each sieve opening size after sieving.

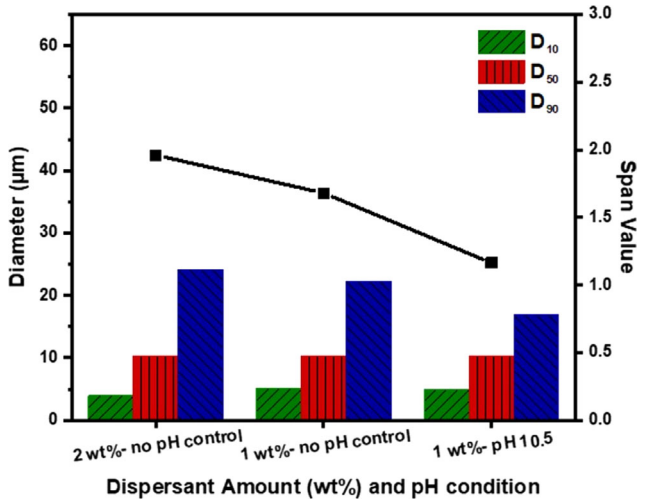

FIGURE 10 D_{10}, D_{50}, D_{90}, and span values of sintered granules with 2 wt% dispersant amount—no pH control, 1 wt% dispersant amount—no pH control, and 1 wt% dispersant amount—pH 10.5.

therefore, the measurement was conducted at 10 mN. The YSZ granules have excellent hardness and elastic modulus of 19.19 and 206.68 GPa, respectively. The hardness and elastic modulus of the epoxy polymer was only 3.63 and 25.78 GPa, respectively. A previous nanoindentation examination of YSZ pellets[40] and coated film[41] showed hardness and Young's modulus of 24.7 and 257 GPa, and of 7.23 and 122 GPa, respectively. In previous research of YSZ granules, the hardness and Young's modulus were 26.77 and 210.19 GPa with 20 μm sized granules[7]; our results are not significantly lower despite being more influenced by the polymer due to a high surface area. This result is a relatively high value, even though the size is smaller and not in film or pellet form; therefore, it can be greatly affected by the polymer wrapping the granule around it.

The details of all the experimental conditions are listed in Table 1. These results have remarkable industrial relevance for applications requiring high-density granulation, such as grinding and milling media. Ultrasmall size of 10 μm YSZ granules with superior sphericity and yield efficiency were synthesized by optimizing the conditions of the slurry. The mechanical strength was sufficiently high for these applications. Moreover, this result presents a new direct approach to spray-drying by optimizing the slurries to control not only the size but also the size distribution.

4 | CONCLUSIONS

The purpose of this study was to determine the influence of slurry conditions on the granule size and size distribution of highly dense YSZ granules synthesized using spray-drying. Furthermore, granules of size 10 μm were synthesized by adjusting the conditions of the slurry with

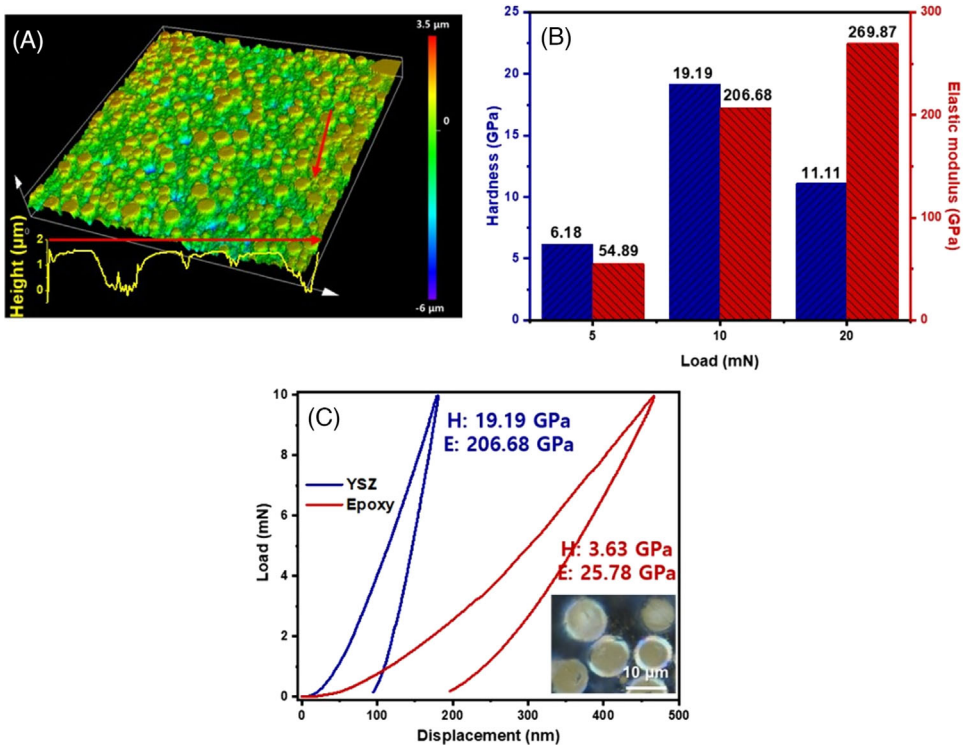

FIGURE 11 (A) 3D surface roughness of the polished surface, (B) hardness and elastic modulus at each load, and (C) load–displacement curve of mounted and polished yttria-stabilized zirconia (YSZ) granules after sintering at the optimized conditions for 10 μm granules and that of epoxy. The inset is an optical image of the measured YSZ granules.

TABLE 1 Summary of the experimental conditions and analysis.

Conditions						D_{50} (yield efficiency)
#	Solid contents (wt%)	Deagglomeration time (h)	Atomizing pressure (kPa)	Dispersant amount (wt%)	pH	
1	65.25	16	250	2	No	8.25
2	75.25	16	250	2	No	9.99
3	77.25	16	250	2	No	13.03
4	80.25	16	250	2	No	31.38
5	77.25	1	250	2	No	15.83
6	77.25	4	250	2	No	13.22
7	77.25	24	250	2	No	11.64
8	77.25	40	250	2	No	11.86
9	77.25	64	250	2	No	10.28 (23.35%)
10	77.25	64	200	2	No	14.93
11	77.25	64	100	2	No	18.89
12	77.25	64	250	1	No	10.25 (67.65%)
13	77.25	64	250	1	10.5	10.20 (80.01%)

the solid contents to form dense granules in deagglomeration, a stable state that maintains high fluidity, and controlling the spray-drying parameters, including the atomizing pressure.

As the solid content of YSZ increased, the size of the granules increased because of the large droplets resulting from the increase in viscosity and reduced shrinkage during evaporation. The size distribution

and density increased but became constant as the solid content increased. A longer deagglomeration time was effective in reducing the size distribution and granule size, but the effect became increasingly insignificant. At the starting point, the viscosity increased with the breaking of the initial conglomeration of the clumped particles to a uniform size; but the longer the time, the viscosity decreased with more improved flowing ability. The density was improved by enhancing the deagglomeration and dispersion as the deagglomeration time increased. Increasing the atomizing pressure reduced the size of the droplet, thus reducing the size of the final granule; however, the size distribution did not change significantly. The stability of the slurry had a significant effect on the size distribution; therefore, it should be adjusted with the proper amount of dispersant and pH. In this study, the degree of stabilization was determined through zeta potential, viscosity, and Turbiscan analyses. The obtained dense YSZ granules showed an average size of 10.6 μm, a high sphericity of 97.17%, significantly improved narrow size distribution with a high fraction yield of 80.01%, and excellent mechanical properties with a hardness of 19.19 GPa and an elastic modulus of 206.68 GPa.

This study shows that the size and distribution of 10 μm granules can be finely adjusted by controlling the conditions of the slurry with a breakthrough in the yield. The yield, which was 20% in our previous study, has dramatically increased to 80.01%. It is expected that the key technology of this study can be applied not only to grinding and milling media but also to various applications requiring granulation.

ACKNOWLEDGMENTS

This work was supported by the Technology Innovation Program (development of 30 μm ceramic beads and reliability evaluation technology, No. 20011008) funded by the Ministry of Trade, Industry & Energy (MOTIE, Korea) and the Korea Institute of Materials Science (KIMS) internal R&D program (No. PNK8140).

CONFLICT OF INTEREST STATEMENT

The authors declare that they have no known conflict of interests or personal relationships that could have influenced the work reported in this study.

ORCID

Hyun-Ae Cha https://orcid.org/0000-0003-3881-8329
Cheol-Woo Ahn https://orcid.org/0000-0002-4667-6079
Jong-Jin Choi https://orcid.org/0000-0001-9598-7933
Do Kyung Kim https://orcid.org/0000-0001-9092-9427

REFERENCES

1. Ghasemi R, Vakilifard H. Plasma-sprayed nanostructured YSZ thermal barrier coatings: thermal insulation capability and adhesion strength. Ceram Int. 2017;43(12):8556–63.
2. Kim BK, Yun JH, Jung WK, Lim CH, Zhang Y, Kim DK. Mitigating grain growth in fully stabilized zirconia via a two-step sintering strategy for aesthetic dental restorations. Int J Appl Ceram Technol. 2022;20:856–68.
3. Judes J, Kamaraj V. Preparation and characterization of yttria stabilized zirconia minispheres by the sol-gel drop generation method. Mater Sci-Pol. 2009;27(2):407–15.
4. Austin L, Shoji K, Luckie PT. The effect of ball size on mill performance. Powder Technol. 1976;14(1):71–9.
5. Bond FC. Grinding ball size selection. Min Eng. 1958;10:592–5.
6. Reed JS. Principles of ceramics processing. New York: Wiley; 1995.
7. Kim Y-R, Lee TW, Park S, Jang J, Ahn C-W, Choi J-J, et al. Supraparticle engineering for highly dense microspheres: yttria-stabilized zirconia with adjustable micromechanical properties. ACS Nano. 2021;15(6):10264–74.
8. Vicent M, Sánchez E, Santacruz I, Moreno R. Dispersion of TiO_2 nanopowders to obtain homogeneous nanostructured granules by spray-drying. J Eur Ceram Soc. 2011;31(8):1413–9.
9. Bertrand G, Filiatre C, Mahdjoub H, Foissy A, Coddet C. Influence of slurry characteristics on the morphology of spray-dried alumina powders. J Eur Ceram Soc. 2003;23(2):263–71.
10. Takahashi H, Shinohara N, Okumiya M, Uematsu K, JunIchiro T, Iwamoto Y, et al. Influence of slurry flocculation on the character and compaction of spray-dried silicon nitride granules. J Am Ceram Soc. 1995;78(4):903–8.
11. Walker WJ Jr, Reed JS, Verma SK. Influence of slurry parameters on the characteristics of spray-dried granules. J Am Ceram Soc. 1999;82(7):1711–9.
12. Tsetsekou A, Agrafiotis C, Leon I, Milias A. Optimization of the rheological properties of alumina slurries for ceramic processing applications Part II: Spray-drying. J Eur Ceram Soc. 2001;21(4):493–506.
13. Marie A, Tourbin M, Robisson A-C, Ablitzer C, Frances C. Wet size measurements for the evaluation of the deagglomeration behaviour of spray-dried alumina powders in suspension. Ceram Int. 2022;48(6):7926–36.
14. Lintingre E, Lequeux F, Talini L, Tsapis N. Control of particle morphology in the spray drying of colloidal suspensions. Soft Matter. 2016;12(36):7435–44.
15. Wang Q, Ge Y, Sun S, Kuang J, Ferreira JM, Cao W. Preparation of dense spherical AlN fillers by aqueous granulation and post-sintering process. Ceram Int. 2017;43(2):2027–32.
16. Raghupathy BP, Binner JG. Spray granulation of nanometric zirconia particles. J Am Ceram Soc. 2011;94(1):42–8.
17. Lukasiewicz SJ. Spray-drying ceramic powders. J Am Ceram Soc. 1989;72(4):617–24.
18. Stunda-Zujeva A, Irbe Z, Berzina-Cimdina L. Controlling the morphology of ceramic and composite powders obtained via spray drying–a review. Ceram Int. 2017;43(15):11543–51.
19. Nandiyanto ABD, Okuyama K. Progress in developing spray-drying methods for the production of controlled morphology particles: from the nanometer to submicrometer size ranges. Adv Powder Technol. 2011;22(1):1–19.

20. Vehring R. Pharmaceutical particle engineering via spray drying. J Pharm Sci Res. 2008;25(5):999–1022.
21. Ramavath P, Papitha R, Ramesh M, Babu PS, Johnson R. Effect of primary particle size on spray formation, morphology and internal structure of alumina granules and elucidation of flowability and compaction behaviour. Process Appl Ceram. 2014;8(2):93–9.
22. Paramita V, Iida K, Yoshii H, Furuta T. Effect of additives on the morphology of spray-dried powder. Dry Technol. 2010;28(3):323–9.
23. Wang A-J, Lu Y-P, Zhu R-F, Li S-T, Ma X-L. Effect of process parameters on the performance of spray dried hydroxyapatite microspheres. Powder Technol. 2009;191(1–2):1–6.
24. Hincapie-Bedoya J, Poblano-Salas C, Moreno-Murguia B, Gutierrez-Perez A, Henao J, Espinosa-Arbelaez D, et al. Effect of the modification of spray drying parameters on the fabrication of bovine-derived hydroxyapatite microspheres for biomedical applications. Mater Today Commun. 2022;31:103838.
25. Vicente J, Pinto J, Menezes J, Gaspar F. Fundamental analysis of particle formation in spray drying. Powder Technol. 2013;247:1–7.
26. Fair GE, Lange FF. Effect of interparticle potential on forming solid, spherical agglomerates during drying. J Am Ceram Soc. 2004;87(1):4–9.
27. Naglieri V, Gutknecht D, Garnier V, Palmero P, Chevalier J, Montanaro L. Optimized slurries for spray drying: different approaches to obtain homogeneous and deformable alumina-zirconia granules. Materials. 2013;6(11):5382–97.
28. Zainuddin MI, Tanaka S, Furushima R, Uematsu K. Correlation between slurry properties and structures and properties of granules. J Eur Ceram Soc. 2010;30(16):3291–6.
29. Mahdjoub H, Roy P, Filiatre C, Bertrand G, Coddet C. The effect of the slurry formulation upon the morphology of spray-dried yttria stabilised zirconia particles. J Eur Ceram Soc. 2003;23(10):1637–48.
30. Bertrand G, Roy P, Filiatre C, Coddet C. Spray-dried ceramic powders: a quantitative correlation between slurry characteristics and shapes of the granules. Chem Eng Sci. 2005;60(1):95–102.
31. Roy P, Bertrand G, Coddet C. Spray drying and sintering of zirconia based hollow powders. Powder Technol. 2005;157(1–3):20–6.
32. Hotza D, Leo A, Sunarso J, Diniz da Costa JC. Effect of nano-Al_2O_3 addition on the densification of YSZ electrolytes. J Nano Res. 2009;6:115–22.
33. Azema N. Sedimentation behaviour study by three optical methods-granulometric and electrophoresis measurements, dispersion optical analyser. Powder Technol. 2006;165(3):133–9.
34. Luo P, Nieh T. Preparing hydroxyapatite powders with controlled morphology. Biomaterials. 1996;17(20):1959–64.
35. Chahal H, Matthews S, Jones M. Effect of process conditions on spray dried calcium carbonate powders for thermal spraying. Ceram Int. 2021;47(1):351–60.
36. Daggupati V, Naterer G, Gabriel K, Gravelsins R, Wang Z. Effects of atomization conditions and flow rates on spray drying for cupric chloride particle formation. Int J Hydrogen Energy. 2011;36(17):11353–9.
37. Chai Z, Ren Y, Zhang R, Feng L, Liu S, Wang Z, et al. Stability and settling performance of coal water slurries under vibration conditions. Powder Technol. 2020;376:351–62.
38. Bechteler C, Kühl H, Girmscheid R. Morphology and structure characterization of ceramic granules. J Eur Ceram Soc. 2020;40(12):4232–42.
39. Yan W, Pun CL, Simon GP. Conditions of applying Oliver–Pharr method to the nanoindentation of particles in composites. Compos Sci Technol. 2012;72(10):1147–52.
40. Fujikane M, Setoyama D, Nagao S, Nowak R, Yamanaka S. Nanoindentation examination of yttria-stabilized zirconia (YSZ) crystal. J Alloys Compd. 2007;431(1–2):250–5.
41. Rauch J, Bolelli G, Killinger A, Gadow R, Cannillo V, Lusvarghi L. Advances in high velocity suspension flame spraying (HVSFS). Surf Coat Technol. 2009;203(15):2131–8.

SUPPORTING INFORMATION

Additional supporting information can be found online in the Supporting Information section at the end of this article.

How to cite this article: Cha H-A, Shin K-C, Son H-J, Hahn B-D, Ahn C-W, Choi J-J, et al. Designing slurry conditions to control size distribution of spray-dried dense YSZ granules. Int J Appl Ceram Technol. 2023;1–13. https://doi.org/10.1111/ijac.14421